

Joint Scalable Coding and Routing for 60 GHz Real-Time Live HD Video Streaming Applications

Joongheon Kim, *Member, IEEE*, Yafei Tian, *Member, IEEE*, Stefan Mangold, *Member, IEEE*,
Andreas F. Molisch, *Fellow, IEEE*

Abstract—Transmission of high-definition (HD) video is a promising application for 60 GHz wireless links, since very high transmission rates (up to several Gbit/s) are possible. In particular we consider a sports stadium broadcasting system where signals from multiple cameras are transmitted to a central location. Due to the high pathloss of 60 GHz radiation over the large distances encountered in this scenario, the use of relays might be required. The current paper analyzes the joint selection of the routes (relays) and the compression rates from the various sources for maximization of the overall video quality. We consider three different scenarios: (i) each source transmits only to one relay and the relay can receive only one data stream, and (ii) each source can transmit only to a single relay, but relays can aggregate streams from different sources and forward to the destination, and (iii) the source can split its data stream into parallel streams, which can be transmitted via different relays to the destination. For each scenario, we derive the mathematical formulations of the optimization problem and re-formulate them as convex mixed-integer programming, which can guarantee optimal solutions. Extensive simulations demonstrate that high-quality transmission is possible for at least ten cameras over distances of 300 m. Furthermore, optimization of the video quality gives results that can significantly outperform algorithms that maximize data rates.

Index Terms—60 GHz, Multi-Gbit/s HD Video Streaming, Wireless Video Quality Maximization, Routing

I. INTRODUCTION

Recently, wireless data transmission and media streaming in the millimeter-wave frequency range have received a lot of attention by the wireless communications and consumer electronics communities. In particular the 60 GHz frequency range is of great interest: a 7 GHz wide band (58-65 GHz) has been made available for unlicensed operation. This large bandwidth enables multi-Gbit/s wireless data transmission [1][2], which enables, in turn, high definition (HD) video streaming in an uncompressed, or less compressed, manner. Therefore, several industry consortia such as WirelessHD [3] and the Wireless Gigabit Alliance (WiGig) [4] have developed related

technical specifications. Also within the IEEE, there are two 60 GHz millimeter-wave standardization activities, i.e., IEEE 802.15.3c Millimeter Wave Alternative PHY [5] (completed in 2009) and IEEE 802.11ad Very High Throughput (VHT) [6], which is currently in the draft stage. First consumer electronics products for short-range transmission (e.g., from Blue-Ray player to HDTV) have recently become available.

In this paper, we analyze 60 GHz for longer-range outdoor applications, i.e., an outdoor sports broadcasting system. In this system, there are multiple wireless HD video cameras in a sports stadium for high-quality real-time broadcasting, all sending their data to a single destination (called "broadcasting center", even though it is the *receiver* of the data streams). To transmit uncompressed HD video streams in real time, a data rate of approximately 1.5 Gbit/s is required.¹ Since the distance between wireless HD video cameras and a broadcasting center is on the order of several hundred meters, the high path-loss at 60 GHz is one of main challenges which leads the limitation of communication ranges, resulting in a reduction of the possible data rate. One promising way to deal with this problem is using *relays* for routing to extend the communication coverage [7]. Increasing the number of relays obviously improves performance, but also increases costs. We are thus interested in finding the tradeoff between performance and number of relays.

We furthermore take the complexity of the antennas into account. In order to compensate for the high pathloss, as well as to reduce interference, high-gain antennas need to be employed. We distinguish between the situations where the antenna can form only a single beam, or multiple beams: (i) If both source and relay have only a single beam, then each source has to select a suitable relay, and the relay can only receive from this particular source. (ii) If sources have single beams, but relays have multiple beams, then the source can transmit only to a single relay, but the relays can receive data from multiple sources and aggregate them before forwarding to the destination. (iii) If also the source has multiple beams, it can split its data stream into multiple parallel streams and send them to the destination via parallel links. If the number of relays is less than the number of sources, then some HD video streams from sources cannot be served by the relays in

Parts of this paper were presented at the 22nd IEEE International Symposium on Personal Indoor and Mobile Radio Communications (PIMRC), Toronto, Canada, 14 September 2011 (refer to [14]).

J. Kim is with the Department of Computer Science, University of Southern California, Los Angeles, CA 90089, USA e-mail: joongheon.kim@usc.edu.

Y. Tian is with the School of Electronics and Information Engineering, Beihang University, Beijing 100191, China e-mail: ytian@buaa.edu.cn.

S. Mangold is with the Disney Research Zurich and the Laboratory for Software Technology, ETH Zurich, 8092 Zurich, Switzerland e-mail: stefan@disneyresearch.com.

A.F. Molisch is with the Ming Hsieh Department of Electrical Engineering, University of Southern California, Los Angeles, CA 90089, USA e-mail: molisch@usc.edu.

¹In a single HD video frame, 1080×1920 pixels exist and each pixel has 24 bit information for RGB format (8 bit for Red, Green and Blue color representation, respectively). In addition, for one second, 30 frames are required in a standard mode. Therefore, approximately 1.5 Gbit/s data rate is required for uncompressed HD video streaming. In addition, for the enhanced mode, 60 frames are required [2]. This paper considers the standard mode but can be extended for the enhanced mode as well.

case (i). In cases (ii) and (iii), appropriate compression and routing of multiple streams via the same relay can be used.

Relay selection of maximization of data throughput has been analyzed in many papers (see Sec. II). However, for video transmission, we are not interested in maximizing the data rate arriving at the destination, but rather the *video quality*, which is related to the data rate in a nonlinear manner. To achieve this goal, the proposed mathematical formulation will select the relays for every single HD video stream and decide the coding rates for each stream. With this given formulation for the three cases, the optimal solutions can be obtained by (i) the theory of unimodular matrices, (ii) a BBLP algorithm [20], or (iii) standard convex optimization techniques.

The remainder of this paper is organized as follows: Section II gives an overview of related work in the literature. Section III explains the details of our reference system, i.e., the outdoor sports broadcasting system using 60 GHz wireless links. Section IV presents the details of the joint scalable video coding and relaying algorithms for maximizing the delivered HD video qualities for the three cases. Section V presents the technique to convert formulated mathematical optimization framework at Section IV as convex programs which can find optimal solutions. Section VI evaluates the performance by simulations and then section VII concludes this paper.

II. RELATED WORK

The topic of wireless network technologies for outdoor sports stadium system was discussed in [19]; however the fundamental setup differs from ours in that [19] considers content distribution to wireless devices of the audience in the stadium, while our investigations are for the real-time streaming service to a broadcasting center in the stadium and from there to audiences at home. In terms of fundamental technology, our research is related to both scalable video coding rate control and relay selection/routing for real-time video transmission.

For the video relaying issue, example publications include [26], [27], [28], [29]. The proposed scheme in [26] addresses opportunistic routing for video transmission over IEEE 802.11 wireless networks under given time constraints. The proposed scheme is efficient in the given multi-hop IEEE 802.11 wireless networks, however, this does not consider the route paths selection problem. Ref. [27], considers distributed video streaming in multi-hop wireless networks. This paper considers network architectures similar to ours (when specialized to the two-hop case), but the proposed algorithm cannot consider the rate control mechanism. The formulation in [28] considers multipath selection for video streaming in a mobile ad-hoc network (MANET) architecture. The main constraint for this algorithm is the interference over the given wireless channel, a factor that does not play a role in our 60 GHz millimeter-wave wireless channel, where the high directionality of the antennas prevents inter-stream interference. The scheme in [29] considers a route selection mechanism for video streaming, but using multi-path video streaming with multicast techniques, which differs from our setup where only a single destination is used. All of these papers [26],

[27], [28], [29] only consider the video multi-hop wireless networks but do not consider the video coding rate control. For the same reason, the rich literature of relay selection and routing of "conventional" data transmission is not applicable to our scenario. In previous research on video streaming, schemes usually considered multipath video data transmission to combat the limited wireless bandwidth [27][28][29]. In addition, some of the research considered retransmission of video signals and tried to reduce transmission time [26]. However, thanks to the very large available bandwidth at 60 GHz, these factors are not longer considered in this paper.

The representative work which considers both rate control and route selection appeared in [31]: In the paper, the proposed algorithm selects the best relays for individual unicast data flows and it selects the corresponding data rates as well. However, the relays in [31] cannot aggregate video streams, which is required when the number of relays is smaller than the number of unicast flows in real-time video streaming applications. In addition, the proposed framework does not consider the properties of video, namely the nonlinear relationship between data rate and video quality because it is for generalized cooperative multi-hop networking systems. In addition, the algorithms in [26], [27], [28], [29], [31] do not care about the wireless channels, thus the given algorithms are not considering the features of millimeter-wave wireless channels. However, they do not consider beamforming for interference suppression, which is an essential part of our architecture. Ref. [32] considers the main features of millimeter-wave wireless communications, i.e., high directionality. It designs the medium access control mechanisms for 60 GHz wireless channels, however, it does not consider the features related to video streaming. In the conference version of this paper [14], we considered the properties of the 60 GHz channel as well as rate control and video quality, but we restricted ourselves to the case that the number of relays exceeds the number of sources.

The comparison studies are summarized in Table I.

III. A REFERENCE SYSTEM MODEL

A. Link Budget Analysis: Capacity Perspective

A link budget analysis [8],[30] provides the fundamental tradeoff between data rate and range that can be achieved. Using Shannon's equation for the capacity

$$C = B \cdot \log_2(1 + \text{SNR}) \quad (1)$$

where SNR is equal to $P_{\text{signal}}/P_{\text{noise}}$ as a linear scale, P_{signal} and P_{noise} stand for the signal power and noise power, respectively. In addition, B stands for bandwidth and is considered as 2.16 GHz respect to WiGig specification [15]. The signal power expressed in dB, $P_{\text{signal, dB}}$, can be computed as follows:

$$P_{\text{signal, dB}} = E + G_r - W - O(m) + F(m) \quad (2)$$

where E stands for the equivalent isotropically radiated power (EIRP), which is limited by frequency regulators to 40 dBm in the USA and 57 dBm in Europe. G_r means the receiver antenna gain; In our system it is set to 40 dB, which corresponds to commercially high-gain 60 GHz outdoor scalar

TABLE I
RELATED WORK COMPARISON TABLE

Consideration Factors	[26]	[27]	[28]	[29]	[31]	[14]	Proposed
Route Selection	○	○	○	○	○	○	○
Rate Allocation	×	×	×	×	○	○	○
Millimeter-Wave Channels	×	×	×	×	×	○	○
Multiple-Antenna Elements	×	×	×	×	×	×	○
Video Streaming	○	○	○	○	×	○	○
Insufficient Number of Relays	-	-	-	-	-	×	○

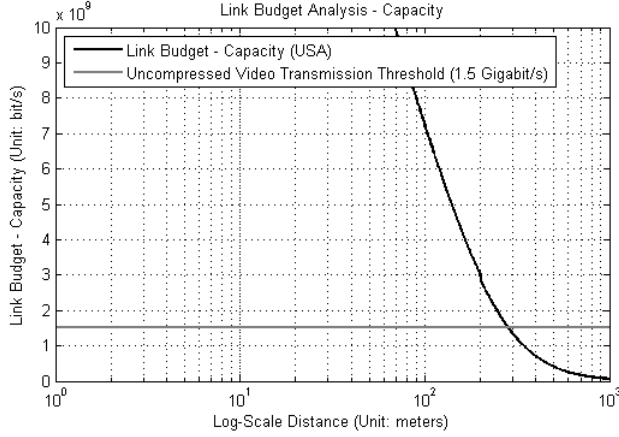


Fig. 1. Link Budget Analysis: Capacity (Unit: bit/s) vs. Log-Scale Distance (Unit: meters)

horn antennas [9], [10], which we propose to achieve large communication range. W presents the shadowing margin and is set as 10 dB; while line-of-sight (LOS) is anticipated for our deployment, obstacles such as passing-by people, raised banners, etc., might attenuate the LOS. $F(m)$ represents the path loss, which depends on the distance (meter) m between transmitter and receiver

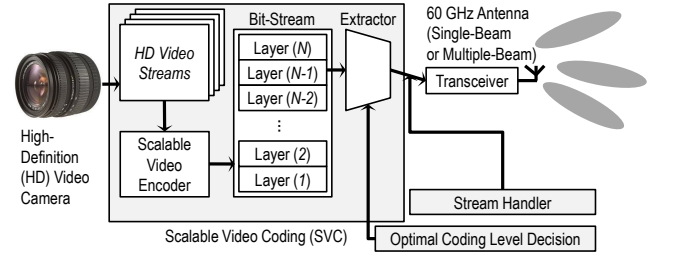
$$F(m) = 10 \log_{10} \left(\frac{\lambda}{4\pi m} \right)^n \quad (3)$$

where n stands for the path loss coefficient and is set as 2.5 [1]. In addition, the wavelength (λ) is 5 millimeter at 60 GHz. $O(m)$ means the oxygen attenuation at distance m , which can be computed as $O(m) = \frac{15}{1000}m$. For $d < 200$ meter, $O(m)$ can be ignored [1]. The noise power in dB, $P_{\text{noise,dB}}$ can be computed as follows:

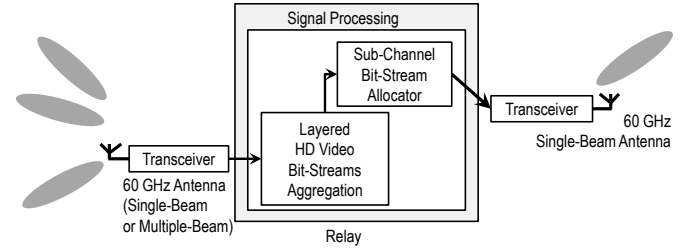
$$P_{\text{noise,dB}} = 10 \log_{10} (k_B T_e \cdot B) + F_N \quad (4)$$

where $k_B T_e$ stands for the noise power spectral density which is -174 dBm/Hz. B presents bandwidth and is set as 2.16 GHz [15]. At last, F_N means the noise figure and is set as 6 dB.

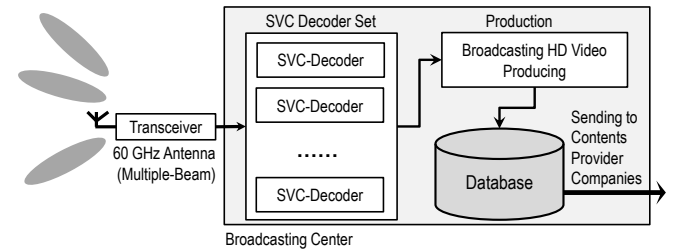
The leads us to conclude that approximately 200 – 300 m is the maximum distance for successful video signal decoding when the maximum data rate of 1.5 Gbit/s is used, as shown in Fig. 1.



(a) Wireless HD Video Camera (Source) Structure



(b) Relay Structure



(c) Broadcasting Center Structure

Fig. 2. System Components

B. Outdoor Broadcasting Systems with 60 GHz Wireless Links

It follows from the above link budget that the assistance of relays is required if the wireless communication range between wireless HD video cameras and a single broadcasting center is approximately more than 200 – 300 m. In the general transport layer mechanisms such as TCP, the congestion control mechanism encounters a number of new problems and suffers from poor performance in multi-hop wireless networks [13]. Thus,

considering a small number of hops is beneficial. Furthermore, the size of sport stadium (i.e., from wireless HD video cameras to the antennas of a broadcasting center) is not more than approximately 500 m (note that, for example, the large side of Los Angeles Memorial Coliseum is approximately 300 m.). Thus, we can safely restrict the number of relays to one, i.e., a two-hop network.

In our outdoor sports broadcasting system, mainly three components which have 60 GHz wireless communication capabilities are existing, i.e., wireless HD video cameras, relays, and a broadcasting center using multiple antennas. As presented in Fig. 2(a), the proposed wireless HD video cameras have scalable video coding (SVC) functionalities that reproduce the real-world analog video signals as layered SVC-coded HD video bit streams. If the achievable rate of a 60 GHz link is sufficient for uncompressed HD video streaming (i.e., 1.5 Gbit/s), then all SVC-coded layers can be transmitted, i.e., the optimal coding level decision module selects all layers. Hence, this can preserve the maximum quality of the delivered video streams. This achievable rate between x and y ($\mathcal{A}_{x \rightarrow y}$) is computed by Eq. (1). If the computed achievable rate is not enough for uncompressed HD video streaming (i.e., less than 1.5 Gbit/s), the optimal coding level decision module has to determine the maximum number of layers, reducing the overall video quality (see below) as discussed in [11],[12].

Each wireless HD video camera can have one of two antenna types: single-beam antennas, or multiple-beam antennas. Single-beam antennas usually are high-gain antenna structures such as horn antennas or Cassegrain antennas. In the single-antennas at sources scenario, all the multiple SVC-coded streams in each camera are assigned to the single antenna, and thus transmitted to the same relay. If the antenna can form N independent beams the multiple SVC-coded streams are divided into N parts and each part is assigned to a beam to be concurrently transmitted. Normally, the multiple beams will be formed by phased-array type antennas, though the use of multiple horn antennas pointing into different directions is possible as well.

If the number of sources exceeds the number of relays, the relays have to have multiple-beam antennas for reception. If the number of sources is smaller than the number of relays, single-beam antennas might be sufficient. In either case, the number of beams for transmission to the broadcast center need not exceed one, since there is only one destination. The destination, however, always has to be able to receive multiple beams simultaneously. Fig. 2(b) shows the proposed architecture when the relays have multiple-beam antennas. The relays use their built-in digital signal processing unit to aggregate the received HD video signals and transmit them towards a broadcasting center via the single antenna. As presented in Fig. 2(c), the proposed broadcasting center has multiple antennas which are facing the relays. We emphasize that due to the narrow beamwidth (1.5-10 degree [9], [10]), of the antennas, multiple streams arriving at the broadcast center do not interfere with each other (and similarly for the relays).

This broadcasting center selects important features of the current real-time sports game. For interactive TV where users can select the camera/viewpoint they prefer, it is often

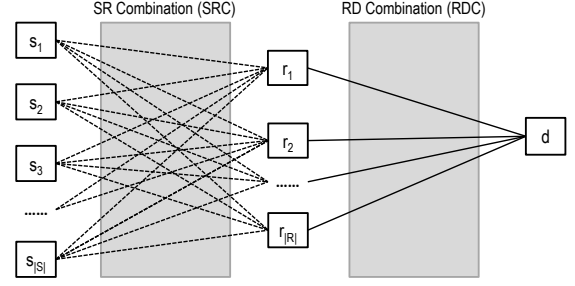


Fig. 3. A System Model

desirable to maximize the overall video quality, subject to constraints on the minimum acceptable quality for each video stream.

IV. JOINT SCALABLE CODING AND ROUTING

Fig. 3 shows the system model with a set of sources \mathcal{S} , a set of relays \mathcal{R} , and a single destination. In the relay-destination combination (RDC) part of Fig. 3, all relays (i.e., $r_1, \dots, r_{|\mathcal{R}|}$) should be connected to the single destination (i.e., the broadcasting center d). Then the maximum achievable rates of all possible relay and destination pairs are computed (denoted as $a_{r_1 \rightarrow d}^{\text{RDC}}, \dots, a_{r_{|\mathcal{R}|} \rightarrow d}^{\text{RDC}}$). We assume that the destination can form a sufficient number of independent beams so that it has no limitations concerning the number of relays from which it can receive. Thus, finding optimal combinations between sources and relays in SRC are considered for the following three scenarios: (i) source and relays have only a single beam (Sec. IV-A), (ii) source has a single beam and relays have multiple beams (Sec. IV-B), and (iii) both sources and relays can form multiple beams (Sec. IV-C).

For all possible scenarios, our objective is the maximization of delivered overall video qualities from sources to the destination, then the relationship between the video qualities and data rates should be defined. The quality of HD video signals is related to the data rate in a nonlinear fashion (i.e., logarithmically and monotonically increasing form). One widely suggested model [16][17][18], is presented at Fig. 4. As shown in Fig. 4, there is no compression loss if the data rate is more than 1.5 Gbit/s because we can exploit uncompressed HD video transmission in a standard mode. We note, however, that this figure might depend on the type of video source - e.g., will be different for fast-moving and slow-moving video. The main features are a monotonic, but sublinear, increase of video quality with data rate.

A. Single-Beam Antennas at Sources and Relays

In this first case, each source has a single-beam antenna and thus can send only to one relay, in addition, each relay also has a single-beam antenna which is for receiving data. Our objective is the maximization of delivered overall video qualities from sources to the destination and the corresponding mathematical formulation is as follows:

$$\max \sum_{j=1}^{|\mathcal{R}|} \sum_{i=1}^{|\mathcal{S}|} f_q \left(\frac{1}{2} a_{s_i \rightarrow r_j}^{\text{SRC}} \right) x_{s_i \rightarrow r_j}^{\text{SRC}} \quad (5)$$

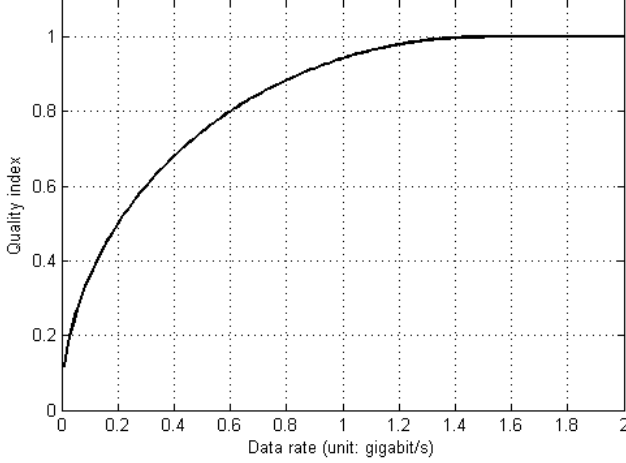


Fig. 4. Generalized relationship between the quality index of transmitted HD video signals and data rates. Based on different kinds of HD video sources, the curve can be varied, but the general form is given as logarithmically and monotonically increasing as proved in [16][17][18].

TABLE II
NOTATIONS USED IN MATHEMATICAL FORMULATION

Notation	Description
\mathcal{S}	Set of sources
\mathcal{R}	Set of relays
d	Destination
s_i	Source i , $\forall i \in \{1, \dots, \mathcal{S} \}$
r_j	Relay j , $\forall j \in \{1, \dots, \mathcal{R} \}$
$\mathcal{A}_{s_i \rightarrow r_j}^{\text{SRC}}$	Max achievable rate between s_i and r_j
$\mathcal{A}_{r_j \rightarrow d}^{\text{RDC}}$	Max achievable rate between r_j and d
$a_{s_i \rightarrow r_j}^{\text{SRC}}$	Data rate between s_i and r_j
$x_{s_i \rightarrow r_j}^{\text{SRC}}$	Connectivity index between s_i and r_j
$\underline{a}_{s_i \rightarrow r_j}^{\text{SRC}}$	Lower bounds of rates at each source s_i for minimum required video quality
$f_q(\cdot)$	Function for the relationship between video quality and data rate (Fig. 4)
B_{s_i}	Number of antenna-beams at s_i
B_{r_j}	Number of antenna-beams at r_j

subject to

$$\sum_{i=1}^{|\mathcal{S}|} a_{s_i \rightarrow r_j}^{\text{SRC}} x_{s_i \rightarrow r_j}^{\text{SRC}} \leq \mathcal{A}_{r_j \rightarrow d}^{\text{RDC}}, \forall j, \quad (6)$$

$$\sum_{i=1}^{|\mathcal{S}|} x_{s_i \rightarrow r_j}^{\text{SRC}} \leq 1, \forall j, \quad (7)$$

$$\sum_{j=1}^{|\mathcal{R}|} x_{s_i \rightarrow r_j}^{\text{SRC}} \leq 1, \forall i, \quad (8)$$

$$\underline{a}_{s_i} \leq \sum_{j=1}^{|\mathcal{R}|} a_{s_i \rightarrow r_j}^{\text{SRC}}, \forall i, \quad (9)$$

$$a_{s_i \rightarrow r_j}^{\text{SRC}} \leq \mathcal{A}_{s_i \rightarrow r_j}^{\text{SRC}}, \forall i, \forall j, \quad (10)$$

$$x_{s_i \rightarrow r_j}^{\text{SRC}} \in \{0, 1\}, \forall i, \forall j, \quad (11)$$

$$x_{r_j \rightarrow d}^{\text{RDC}} = 1, \forall j, \quad (12)$$

where the used notation is listed in Table II. In this formulation, i and j are the indices of sources and relays where $i \in \{1, \dots, |\mathcal{S}|\}$ and $j \in \{1, \dots, |\mathcal{R}|\}$. If the connectivity between s_i and r_j is active (i.e., if source s_i selects relay r_j), then the corresponding $x_{s_i \rightarrow r_j}^{\text{SRC}}$ is 1 by Eq. (11). Otherwise, $x_{s_i \rightarrow r_j}^{\text{SRC}}$ is 0 by Eq. (11). The given relays should be connected to the destination, thus, $x_{r_j \rightarrow d}^{\text{RDC}} = 1$ as shown in Eq. (12). The $\mathcal{A}_{s_i \rightarrow r_j}^{\text{SRC}}$ and $\mathcal{A}_{r_j \rightarrow d}^{\text{RDC}}$ are maximum achievable rates for the corresponding wireless links and computed by Eq. (1). In addition, the desired data rates between s_i and r_j should be less than the computed $\mathcal{A}_{s_i \rightarrow r_j}^{\text{SRC}}$ as shown in Eq. (10). As shown in Eq. (9), we have to respect the required minimum data rates for each flow (i.e., \underline{a}_{s_i} , $\forall s_i$) to guarantee the required minimum video qualities for each flow (i.e., $f_q(\underline{a}_{s_i})$, $\forall s_i$). In this formulation, $\mathcal{A}_{s_i \rightarrow r_j}^{\text{SRC}}$ from s_i to r_j and $\mathcal{A}_{r_j \rightarrow d}^{\text{RDC}}$ from r_j to d are fixed values due to the fact that the sources and relays are not mobile and the channel is not time-varying.

Since each relay can receive one video stream, and these have to go to the destination via the wireless link with a limited capacity $\mathcal{A}_{r_j \rightarrow d}^{\text{RDC}}$, Eq. (6) follows. For each individual source, there is at most one outgoing flow toward relays because the sources have single-beam antennas, as formulated in Eq. (8). Similarly, each relay can form only one beam in receiving mode, thus the number of incoming flows from sources can be at most one as formulated in Eq. (7). Finally, Eq. (5) describes the objective of finding the set of pairs between sources and relays as well as finding the corresponding data rates for maximizing the total video quality and the corresponding data rate value becomes half due to half-duplex constraint.

The set of equations Eqs. (5 - 12) can be solved by the method of Sec. V. Alternatively, we note that this setup is a special case of a scenario treated in our conference paper [14]. In that paper, the proposed algorithm addresses the relay selection and cooperative communication scheme selection for a situation where several source-destination unicast pairs exist, and furthermore transmission between the pairs can occur not only using decode-and-forward, but also amplify-and-forward (AF), and non-cooperative communications (non-CC) direct transmission. In the system configuration of [14], an algorithm selects the relay node and transmission mode for every single unicast pair in terms of maximization of overall transferred video qualities. Thus, the current scenario can be seen as a special case of the scenario in [14]. Thus, our mathematical formulation, which show that the connectivity matrix is totally unimodular, which in turn guarantees polynomial-time solutions (i.e., a closed-form solution is possible), can be applied also in this case. On the other hand, this framework cannot be easily generalized to the multi-beam scenarios.

The proposed scheme in this section is meaningful under the assumption that the number of relays is larger or equal to the number of sources; otherwise, some video flows from sources cannot reach to the destination. However, positioning lots of relays obviously increases the cost of network system configuration. To deal with this problem, more advanced

relay architectures, which allow multiple-beam antennas, are proposed and the schemes for this case are discussed in the following two sections.

B. Single-Beam Antennas at Sources and Multiple-Beam Antennas at Relays

Each source has a single-beam antenna and thus can send only to one relay, while relays can aggregate streams from different sources. Therefore, the relays have multiple-beam antennas, the constraint Eq. (7) is updated to allow multiple incoming flows as follows:

$$\sum_{i=1}^{|\mathcal{S}|} x_{s_i \rightarrow r_j}^{\text{SRC}} \leq B_{r_j}, \forall j, \quad (13)$$

where B_{r_j} stands for the number of antenna-beams at relay $j, \forall j \in \{1, \dots, |\mathcal{R}|\}$. Thus the corresponding formulation for maximizing overall qualities of received HD video streams from sources to a destination is as follows:

$$\max \sum_{j=1}^{|\mathcal{R}|} \sum_{i=1}^{|\mathcal{S}|} f_q \left(\frac{1}{2} a_{s_i \rightarrow r_j}^{\text{SRC}} \right) x_{s_i \rightarrow r_j}^{\text{SRC}} \quad (14)$$

subject to

$$\sum_{i=1}^{|\mathcal{S}|} a_{s_i \rightarrow r_j}^{\text{SRC}} x_{s_i \rightarrow r_j}^{\text{SRC}} \leq \mathcal{A}_{r_j \rightarrow d}^{\text{RDC}}, \forall j, \quad (15)$$

$$\sum_{i=1}^{|\mathcal{S}|} x_{s_i \rightarrow r_j}^{\text{SRC}} \leq B_j^r, \forall j, \quad (16)$$

$$\sum_{j=1}^{|\mathcal{R}|} x_{s_i \rightarrow r_j}^{\text{SRC}} \leq 1, \forall i, \quad (17)$$

$$a_{s_i} \leq \sum_{j=1}^{|\mathcal{R}|} a_{s_i \rightarrow r_j}^{\text{SRC}}, \forall i, \quad (18)$$

$$a_{s_i \rightarrow r_j}^{\text{SRC}} \leq \mathcal{A}_{s_i \rightarrow r_j}^{\text{SRC}}, \forall i, \forall j, \quad (19)$$

$$x_{s_i \rightarrow r_j}^{\text{SRC}} \in \{0, 1\}, \forall i, \forall j, \quad (20)$$

$$x_{r_j \rightarrow d}^{\text{RDC}} = 1, \forall j, \quad (21)$$

where the used notations are listed in Table II. In this formulation, the meaning of equation are same with the formulation at Section IV-A except Eq. (16). In this section, for each relay, for the receive model, each antenna can form $|\mathcal{S}|$ beams, thus the number of incoming flows from sources can be at most $|\mathcal{S}|$ as formulated in Eq. (16).

C. Multiple-Beam Antennas at Source and Relays

When the sources have multiple-beam antennas, the constraint Eq. (17) is updated to allow multiple outgoing flows for all sources as follows:

$$\sum_{j=1}^{|\mathcal{R}|} x_{s_i \rightarrow r_j}^{\text{SRC}} \leq B_{s_i}, \forall i. \quad (22)$$

where B_{s_i} stands for the number of antenna-beams at source $i, \forall i \in \{1, \dots, |\mathcal{S}|\}$. At last, each wireless HD video camera can have an individual lower bound on the video quality. In Sec. IV-B, a_{s_i} represents the individual video quality lower bound at each source s_i .

Summarizing, the mathematical formulation can be again written as follows:

$$\max \sum_{j=1}^{|\mathcal{R}|} \sum_{i=1}^{|\mathcal{S}|} f_q \left(\frac{1}{2} a_{s_i \rightarrow r_j}^{\text{SRC}} \right) x_{s_i \rightarrow r_j}^{\text{SRC}} \quad (23)$$

subject to

$$\sum_{i=1}^{|\mathcal{S}|} a_{s_i \rightarrow r_j}^{\text{SRC}} x_{s_i \rightarrow r_j}^{\text{SRC}} \leq \mathcal{A}_{r_j \rightarrow d}^{\text{RDC}}, \forall j, \quad (24)$$

$$\sum_{i=1}^{|\mathcal{S}|} x_{s_i \rightarrow r_j}^{\text{SRC}} \leq B_{r_j}, \forall j, \quad (25)$$

$$\sum_{j=1}^{|\mathcal{R}|} x_{s_i \rightarrow r_j}^{\text{SRC}} \leq B_{s_i}, \forall i, \quad (26)$$

$$a_{s_i} \leq \sum_{j=1}^{|\mathcal{R}|} a_{s_i \rightarrow r_j}^{\text{SRC}}, \forall i, \quad (27)$$

$$a_{s_i \rightarrow r_j}^{\text{SRC}} \leq \mathcal{A}_{s_i \rightarrow r_j}^{\text{SRC}}, \forall i, \forall j, \quad (28)$$

$$x_{s_i \rightarrow r_j}^{\text{SRC}} \in \{0, 1\}, \forall i, \forall j, \quad (29)$$

$$x_{r_j \rightarrow d}^{\text{RDC}} = 1, \forall j, \quad (30)$$

D. Discussion

In some cases direct transmission from source to a broadcasting center can guarantee better video quality, then transmission via relay. This can be incorporated in our framework by placing a virtual relay (denoted as $r_{(v,j)}$ in this subsection) at a location very close to the destination, and letting the capacity between the relay and a broadcasting center be infinity (i.e., $\mathcal{A}_{r_{(v,j)} \rightarrow d}^{\text{RDC}} = \infty$), while the achievable capacity between source and relay is $2 \cdot \mathcal{A}_{s_i \rightarrow r_{(v,j)}}^{\text{SRC}}$, where the factor 2 reflects the fact that there is no half-duplex penalty in direct transmission.

V. RE-FORMULATION: CONVEX FORM

The proposed three mathematical formulations can be non-convex mixed-integer nonlinear programs (MINLP) even though the quality function has a convex form (Fig. 4) as shown in following theorem.

Theorem 1: The three optimization formulation appeared in Section IV can be a non-convex MINLP.

Proof: If there exists a quality function which has logarithmically and monotonically increasing property (Fig. 4) which can make our designed mathematical formulation be non-convex MINLP, then the corresponding formulation is non-convex. Then, following equation is one example of possible quality index function:

$$f_q(a) = \frac{1}{\log_\beta(a_{\max} + 1)} \log_\beta(a + 1) \quad (31)$$

β is a base ($1 < \beta$), a_{\max} is a desired data rate for uncompressed video transmission (1.5 Gbit/s in a standard mode), and a is a given data rate. This proof considers the scenario of one-source and one-relay, which is the simplest case. In this case the objective function becomes

$$f(a_{s_i \rightarrow r_j}^{\text{SRC}}, x_{s_i \rightarrow r_j}^{\text{SRC}}) \triangleq f_q(a_{s_i \rightarrow r_j}^{\text{SRC}}) x_{s_i \rightarrow r_j}^{\text{SRC}} \quad (32)$$

$$= \mathcal{K} \log_{\beta} \left(a_{s_i \rightarrow r_j}^{\text{SRC}} + 1 \right) x_{s_i \rightarrow r_j}^{\text{SRC}} \quad (33)$$

where $\mathcal{K} = \frac{1}{\log_{\beta}(a_{\max}+1)}$ is constant and $\forall i \in \{1 \dots, |S|\}, \forall j \in \{1, \dots, |\mathcal{R}|\}$. To show that this given equation is non-convex, the second-order Hessian of this given real function should be non positive definite [22]. The Hessian $\nabla^2 f(a_{s_i \rightarrow r_j}^{\text{SRC}}, x_{s_i \rightarrow r_j}^{\text{SRC}})$ is:

$$\begin{bmatrix} 0 & \frac{\mathcal{K}}{\ln \beta} \cdot \frac{1}{a_{s_i \rightarrow r_j}^{\text{SRC}} + 1} \\ \frac{\mathcal{K}}{\ln \beta} \cdot \frac{1}{a_{s_i \rightarrow r_j}^{\text{SRC}} + 1} & -x_{s_i \rightarrow r_j}^{\text{SRC}} \cdot \left(\frac{\mathcal{K}}{\ln \beta} \cdot \left(\frac{1}{a_{s_i \rightarrow r_j}^{\text{SRC}} + 1} \right)^2 \right) \end{bmatrix} \quad (34)$$

and then the corresponding two eigenvalues are

$$\frac{1}{2} \mathcal{M} \pm \frac{1}{2} \left\{ \mathcal{M}^2 + 4 \left(\frac{\mathcal{K}}{\ln \beta} \cdot \frac{1}{a_{s_i \rightarrow r_j}^{\text{SRC}} + 1} \right)^2 \right\}^{0.5} \quad (35)$$

where $\mathcal{M} = -x_{s_i \rightarrow r_j}^{\text{SRC}} \cdot \frac{\mathcal{K}}{\ln \beta} \cdot \left(\frac{1}{a_{s_i \rightarrow r_j}^{\text{SRC}} + 1} \right)^2$, $0 \leq a_{s_i \rightarrow r_j}^{\text{SRC}} \leq 1.5$, and $0 \leq x_{s_i \rightarrow r_j}^{\text{SRC}} \leq 1$. These values are not all positive, which shows that the Hessian is not positive definite, which proves that the optimization function is non-convex. ■

For non-convex MINLP, heuristic searches can find approximate solutions but cannot guarantee optimality. Among well-known approximation algorithms, branch-and-refine based algorithms show relatively better performance for non-convex MINLP problems [23]. The detailed procedure of the branch-and-refine based algorithms is as follows: First, the integer terms are relaxed (relaxation), i.e., $x_{s_i \rightarrow r_j}^{\text{SRC}} \in \{0, 1\}$ is converted to $0 \leq x_{s_i \rightarrow r_j}^{\text{SRC}} \leq 1$. After that, the special ordered sets (SOS) approximation is used for a linear approximation. This segments the multi-dimensional space of the given objective function into multiple small triangular regions, each of which is plane; in other words, the triangle regions approximate the multi-dimensional surface of the objective function. For every single triangle region, optimum solutions can be obtained by running a simplex based algorithm. Then, we run the branch-and-bound algorithm to find integer solutions for $x_{s_i \rightarrow r_j}^{\text{SRC}}$ for each single triangle region. Thus finally the optimum value is selected among the solutions on the triangles. However, the branch-and-refine algorithm cannot guarantee the optimum solutions in a non-convex MINLP. First of all, if the segmentation into plane triangle regions is rough, then the approximated planes are not precise enough to get the optimum solutions. If the segmentation into plane triangle regions is too fine, the runtime becomes excessive, since the simplex algorithm should be operated for every single triangular region. In conclusion, using branch-and-refine based algorithm provides an approximation but cannot guarantee the optimum solutions and, moreover, this algorithm cannot find bounds on the

approximation errors.

Therefore, if there is a way to convert the non-convex MINLP to convex MINLP, then re-formulated convex MINLP can guarantee the optimum solution. With the following Theorem, our non-convex MINLP can be re-formulated as a convex program form.

Theorem 2: For the given non-convex MINLP formulation in Section IV, introducing

$$a_{s_i \rightarrow r_j}^{\text{SRC}} \leq \mathcal{A}_{s_i \rightarrow r_j}^{\text{SRC}} \cdot x_{s_i \rightarrow r_j}^{\text{SRC}}, \forall i, \forall j \quad (36)$$

instead of Eq. (19), Eq. (10), Eq. (28) makes the formulation a convex program.

Proof: For the non-convex MINLP formulation in Section IV, $x_{s_i \rightarrow r_j}^{\text{SRC}} = 0$ means the link is disconnected. Thus the corresponding rate becomes 0 and Eq. (36) leads to the same result when $x_{s_i \rightarrow r_j}^{\text{SRC}} = 0$, i.e.,

$$a_{s_i \rightarrow r_j}^{\text{SRC}} \leq \mathcal{A}_{s_i \rightarrow r_j}^{\text{SRC}} \cdot 0, \forall i, \forall j, \quad (37)$$

thus,

$$a_{s_i \rightarrow r_j}^{\text{SRC}} \leq 0, \forall i, \forall j. \quad (38)$$

and then $a_{s_i \rightarrow r_j}^{\text{SRC}}$ is equal to 0 because $a_{s_i \rightarrow r_j}^{\text{SRC}}$ is non-negative. Otherwise, if $x_{s_i \rightarrow r_j}^{\text{SRC}} = 1$, then this term is equivalent to Eq. (19), Eq. (10), and Eq. (28). Therefore, in turn, Eq. (5), Eq. (14), Eq. (23) are also updated as

$$\max \sum_{j=1}^{|\mathcal{R}|} \sum_{i=1}^{|S|} f_q \left(\frac{1}{2} a_{s_i \rightarrow r_j}^{\text{SRC}} \right) \quad (39)$$

and Eq. (6), Eq. (15), and Eq. (24) are updated as follows as well:

$$\sum_{i=1}^{|S|} a_{s_i \rightarrow r_j}^{\text{SRC}} \leq \mathcal{A}_{r_j \rightarrow d}^{\text{RDC}}, \forall j. \quad (40)$$

Then there are no non-convex terms in the proposed mathematical programs. ■

Summarizing, the optimization problem can be reformulated as follows. For the single-beam antennas at sources and relays:

$$\max \sum_{j=1}^{|\mathcal{R}|} \sum_{i=1}^{|S|} f_q \left(\frac{1}{2} a_{s_i \rightarrow r_j}^{\text{SRC}} \right) \quad (41)$$

subject to

$$\sum_{i=1}^{|S|} a_{s_i \rightarrow r_j}^{\text{SRC}} \leq \mathcal{A}_{r_j \rightarrow d}^{\text{RDC}}, \forall j, \quad (42)$$

$$\sum_{i=1}^{|S|} x_{s_i \rightarrow r_j}^{\text{SRC}} \leq 1, \forall j, \quad (43)$$

$$\sum_{j=1}^{|\mathcal{R}|} x_{s_i \rightarrow r_j}^{\text{SRC}} \leq 1, \forall i, \quad (44)$$

$$a_{s_i} \leq \sum_{j=1}^{|\mathcal{R}|} a_{s_i \rightarrow r_j}^{\text{SRC}}, \forall i, \quad (45)$$

$$a_{s_i \rightarrow r_j}^{\text{SRC}} \leq \mathcal{A}_{s_i \rightarrow r_j}^{\text{SRC}} \cdot x_{s_i \rightarrow r_j}^{\text{SRC}}, \forall i, \forall j, \quad (46)$$

$$x_{s_i \rightarrow r_j}^{\text{SRC}} \in \{0, 1\}, \forall i, \forall j, \quad (47)$$

$$x_{r_j \rightarrow d}^{\text{RDC}} = 1, \forall j, \quad (48)$$

where $\forall i \in \{1, \dots, |\mathcal{S}|\}, \forall j \in \{1, \dots, |\mathcal{R}|\}$. In addition, for the single-beam antennas at sources and multiple-beam antennas at relays case:

$$\max \sum_{j=1}^{|\mathcal{R}|} \sum_{i=1}^{|\mathcal{S}|} f_q \left(\frac{1}{2} a_{s_i \rightarrow r_j}^{\text{SRC}} \right) \quad (49)$$

subject to

$$\sum_{i=1}^{|\mathcal{S}|} a_{s_i \rightarrow r_j}^{\text{SRC}} \leq \mathcal{A}_{r_j \rightarrow d}^{\text{RDC}}, \forall j, \quad (50)$$

$$\sum_{i=1}^{|\mathcal{S}|} x_{s_i \rightarrow r_j}^{\text{SRC}} \leq B_{r_j}, \forall j, \quad (51)$$

$$\sum_{j=1}^{|\mathcal{R}|} x_{s_i \rightarrow r_j}^{\text{SRC}} \leq 1, \forall i, \quad (52)$$

$$a_{s_i} \leq \sum_{j=1}^{|\mathcal{R}|} a_{s_i \rightarrow r_j}^{\text{SRC}}, \forall i, \quad (53)$$

$$a_{s_i \rightarrow r_j}^{\text{SRC}} \leq \mathcal{A}_{s_i \rightarrow r_j}^{\text{SRC}} \cdot x_{s_i \rightarrow r_j}^{\text{SRC}}, \forall i, \forall j, \quad (54)$$

$$x_{s_i \rightarrow r_j}^{\text{SRC}} \in \{0, 1\}, \forall i, \forall j, \quad (55)$$

$$x_{r_j \rightarrow d}^{\text{RDC}} = 1, \forall j, \quad (56)$$

where $\forall i \in \{1, \dots, |\mathcal{S}|\}, \forall j \in \{1, \dots, |\mathcal{R}|\}$ and finally for the multiple-beam antennas at source and relays case, the updated convex program is as follows:

$$\max \sum_{j=1}^{|\mathcal{R}|} \sum_{i=1}^{|\mathcal{S}|} f_q \left(\frac{1}{2} a_{s_i \rightarrow r_j}^{\text{SRC}} \right) \quad (57)$$

subject to

$$\sum_{i=1}^{|\mathcal{S}|} a_{s_i \rightarrow r_j}^{\text{SRC}} \leq \mathcal{A}_{r_j \rightarrow d}^{\text{RDC}}, \forall j, \quad (58)$$

$$\sum_{i=1}^{|\mathcal{S}|} x_{s_i \rightarrow r_j}^{\text{SRC}} \leq B_{r_j}, \forall j, \quad (59)$$

$$\sum_{j=1}^{|\mathcal{R}|} x_{s_i \rightarrow r_j}^{\text{SRC}} \leq B_{s_i}, \forall i, \quad (60)$$

$$a_{s_i} \leq \sum_{j=1}^{|\mathcal{R}|} a_{s_i \rightarrow r_j}^{\text{SRC}}, \forall i, \quad (61)$$

$$a_{s_i \rightarrow r_j}^{\text{SRC}} \leq \mathcal{A}_{s_i \rightarrow r_j}^{\text{SRC}} \cdot x_{s_i \rightarrow r_j}^{\text{SRC}}, \forall i, \forall j, \quad (62)$$

$$x_{s_i \rightarrow r_j}^{\text{SRC}} \in \{0, 1\}, \forall i, \forall j, \quad (63)$$

$$x_{r_j \rightarrow d}^{\text{RDC}} = 1, \forall j. \quad (64)$$

where $\forall i \in \{1, \dots, |\mathcal{S}|\}, \forall j \in \{1, \dots, |\mathcal{R}|\}$.

With these given convex programs, the given integer constraints, i.e., $x_{s_i \rightarrow r_j}^{\text{SRC}} \in \{0, 1\}$ are relaxed as $0 \leq x_{s_i \rightarrow r_j}^{\text{SRC}} \leq 1$, $\forall i \in \{1, \dots, |\mathcal{S}|\}, \forall j \in \{1, \dots, |\mathcal{R}|\}$. Then the convex programs are solved using CVX which is the most popular matlab-based software for solving convex optimization problems [25].

VI. PERFORMANCE EVALUATION

To verify the superior performance of our proposed scheme, i.e., joint HD video coding rate decision and relay selection/routing scheme under the consideration of overall video quality maximization (named VQM), we compare it with the following two schemes:

- The joint HD video coding rate decision and relay selection/routing scheme under the consideration of *sum rate maximization*. In this case, the proposed three objective functions, i.e., Eq. (41), Eq. (49), Eq. (57), should be updates as follows:

$$\max \sum_{j=1}^{|\mathcal{R}|} \sum_{i=1}^{|\mathcal{S}|} \frac{1}{2} a_{s_i \rightarrow r_j}^{\text{SRC}} \quad (65)$$

due to the fact that the quality function (Fig. 4) is no longer considered. Note that the half-duplex constraint is still existing. This method is named as SRM, i.e., sum rate maximization.

- The scheme proposed in [31], which is a highly efficient algorithm that considers relay selection/routing and rate allocation at the same time. In order to enable fair comparisons, we adapt the scheme to our outdoor-stadium architecture (one-tier relay) and allow only decode-and-forward relaying. Lastly, Ref. [31] has same number of sources and destinations, however, to unify the network setup for performance comparison, all the given destinations are located at the same location and operate as a single destination with multiple antenna elements. This method is named as JRSR, i.e., joint relay selection and routing.

With these given three schemes, i.e., VQM, SRM, JRSR, overall delivered video quality values are simulated in the reference models shown in Fig. 5. The sources (HD cameras) are uniformly distributed on top of the stadium. Between stadium and broadcasting center, multiple relays are uniformly deployed along a line. To vary the simulation scenarios, we consider this line to be near the sources (Scenario A), in the middle between sources and broadcast center (Scenario B), and near the broadcast center (Scenario C). Lastly, we also consider a scenario where the relay position is uniformly randomly distributed. In Scenario A, there is a higher probability that the relay- to - destination link might be the bottleneck, while Scenario C obviously has the source-relay link as its bottleneck.

In addition, for the simulation studies with multiple antenna-beams at sources or relays, the number of relays and the number of sources are set as $|\mathcal{S}|$ and $|\mathcal{R}|$, respectively.

As our performance measure we consider the cumulative probability distribution of the aggregate video quality. We will in the following subsections show results for a fixed number

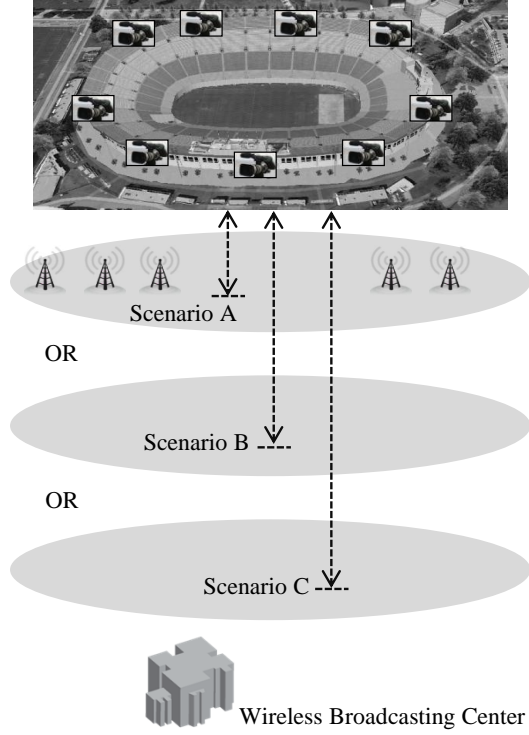


Fig. 5. Performance Evaluation Simulation Setup: Wireless HD video cameras are uniformly distributed on top of the stadium. There is on broadcasting center at bottom. Between wireless video cameras on top of stadium and broadcasting center, relays are uniformly and linearly deployed. To vary simulation setting, the deployment of relays has three different types: the relays are distributed near cameras (Scenario A), in the middle of cameras (on top of stadium) and broadcasting center (Scenario B), and near broadcasting center (Scenario C). The figure of stadium is Los Angeles Memorial Coliseum from [33].

of relays ($|\mathcal{R}| = 10$) and various number of sources ($|\mathcal{S}| = 5, 10, 15$) at first (Sec. VI-A). The cdf is obtained as follows: we consider multiple realizations of the deployment of sources and relays (for a fixed scenario and number of relays, but random relay location according to the location pdf of a given scenario). For each such realization, we optimize coding rates and relay selection; thus each run gives us one realization of the aggregate video quality. We finally plot the cdf of this quality. For the simulation of VQM, the lower bounds of each flow are set as 0.75, i.e., all \underline{a}_{s_i} where $\forall i \in \{1, \dots, |\mathcal{S}|\}$ are all set to 0.75 (Unit: Gbit/s) in a standard mode (i.e., 50% of 1.5 Gbit/s). Then, Section VI-C shows the performance behavior by various lower bound setting is observed.

A. CDF of Aggregate Video Quality – Fixed Number of Relays and Various Number of Sources

1) *Single-Beam Antennas at Sources and Relays*: Fig. 6 presents the cases that the number of sources is smaller, equal, or larger than the number of relays (i.e., $|\mathcal{S}| = 5, 10, 15$, and $|\mathcal{R}| = 10$). We see that SRM and JRSR show the same performance because they are equivalent with the given constraints for single-beam antennas at sources and relays. For the case of 5 sources, we also see that with the proposed VQM, the aggregate video quality is within 5% of its maximum for

TABLE III
EXPECTATION OF ACHIEVED AGGREGATED VIDEO QUALITY FOR SINGLE-BEAM ANTENNAS AT SOURCES AND RELAYS CASE

$ \mathcal{S} $	$ \mathcal{R} $	Scenario	VQM	SRM	JRSR
5	10	A	4.1469	3.3313	3.3313
5	10	B	4.9175	4.1650	4.1650
5	10	C	4.4093	3.6315	3.6315
5	10	Random	4.4262	3.6534	3.6534
10	5	A	4.1520	3.3522	3.3522
10	5	B	4.9216	4.1817	4.1817
10	5	C	4.4138	3.6499	3.6499
10	5	Random	4.4299	3.6707	3.6707
10	10	A	8.7400	5.4825	5.4825
10	10	B	9.5420	6.3360	6.3360
10	10	C	8.9462	5.7946	5.7946
10	10	Random	9.1651	5.2044	5.2044
10	15	A	8.7804	5.6326	5.6326
10	15	B	9.7914	6.4561	6.4561
10	15	C	9.1806	5.9267	5.9267
10	15	Random	9.1919	5.8532	5.8532
15	10	A	9.1075	6.4825	6.4825
15	10	B	9.8860	7.3760	7.3760
15	10	C	9.3746	6.8386	6.8386
15	10	Random	9.3914	6.8510	6.8510

83% of simulation runs in Scenario A, 98% of simulation runs in Scenario B, 88% of simulation runs in Scenario C and 89% of random deployment. Note that the given number of sources is 5, thus, the maximum achievable video quality is 5 due to the fact that the maximum video quality index in each flow is normalized as 1 (refer to Fig. 4). We also find that deployment scenario Scenario B can obtain more quality than the others deployment scenarios since it best balances capacity constraints on the source-relay and relay-destination links. The mean achieved aggregate video qualities are also give in Table III. For the case of 10 or 15 sources, the maximum achievable aggregated video quality is 10 because the given number of relays is 10 which takes a role of threshold of the delivered quality.

2) *Single-Beam Antennas at Sources and Multiple-Beam Antennas at Relays*: Fig. 7 presents plots similar to Fig. 6, but now with multiple-beam antennas at the relays, so that the relays can aggregate and combine video streams from different sources.

In this case there exist performance difference between SRM and JRSR. The latter, by design, does not allow the exploitation of the multiple-beam antennas at relays, and thus shows worse performance. As a matter of fact, it has the same performance as with single-beam antennas at sources and relays case if the network configuration is equivalent. This fact will even holds in the case of multiple-beam antennas at sources and relays. We furthermore see that again SRM shows lower performance than VQM due to the fact that SRM aims to the maximization of sum data rates, while VQM aims to maximize the overall delivered video quality.

We also see that for the case that the number of relays is sufficient (larger than or equal to the number of sources), the

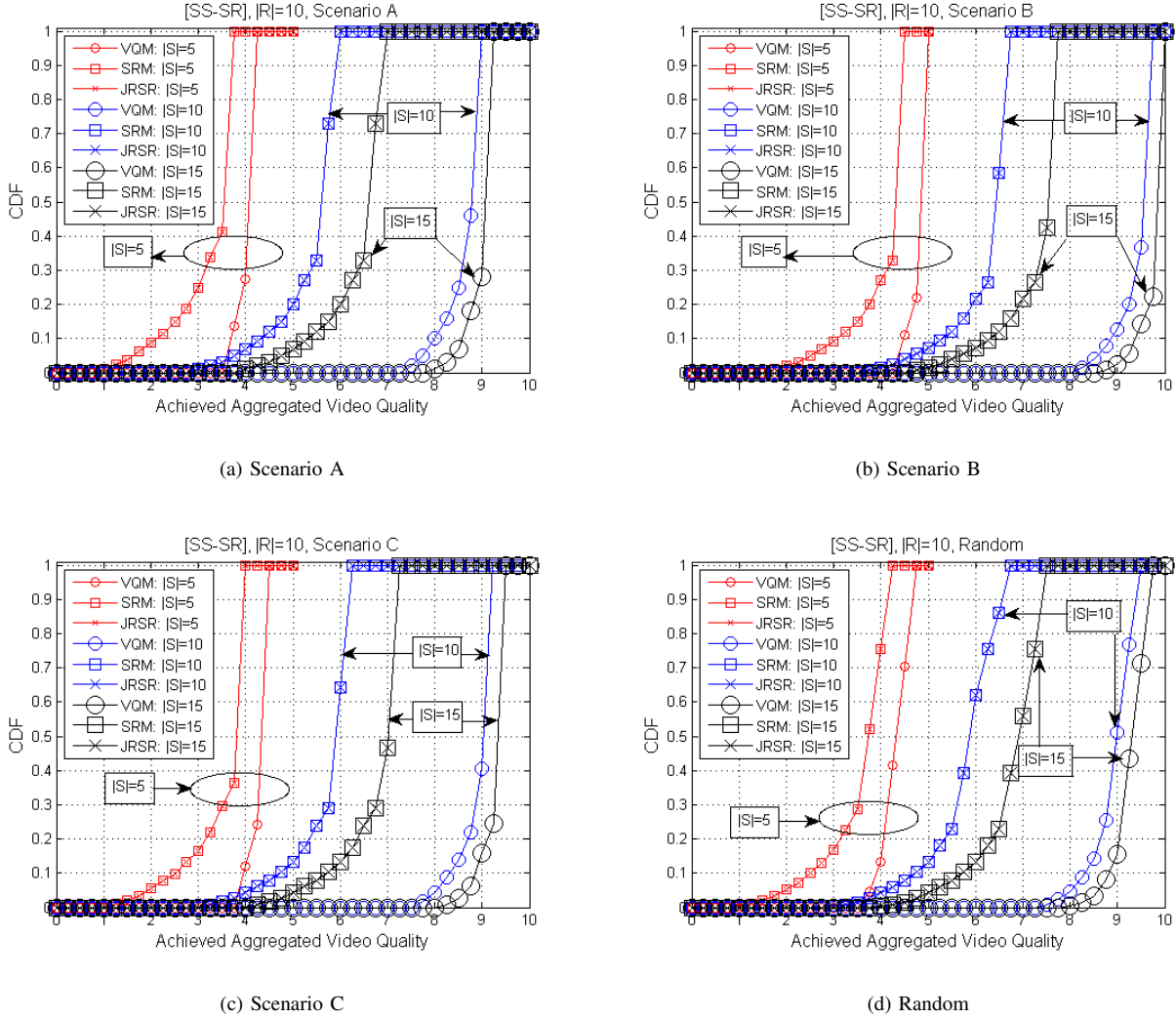


Fig. 6. Simulation Result for Single-Beam Antennas at Sources and Relays: Various Number of Sources ($|S| = 5, 10, 15$) and Fixed Number of Relays ($|R| = 10$)

achieved video quality is not fundamentally different from the case with single-beam antennas at the relays. However, this changes when the number of relays is not sufficient (i.e., $|S| = 15$, $|R| = 10$). We can now achieve aggregate video quality larger than 10 as some streams can be compressed with little video quality loss and forwarded by the same relay. Nonideal performance is mainly caused by the capacity limitations of the relay-destination links. These limitations have more impact on scenarios A and B than in Scenario C.

3) *Multiple-Beam Antennas at Sources and Relays:* For multiple-beam antennas at both sources and relays, VQM and SRM have better performance than the case of single-beam antennas at sources, while JRSR has same performance with the case of single-beam antennas as described above. We also note that in this case, the optimization for SRM can be solved by a maximum flow formulation as shown in Appendix A. With the benefit of multiple-beam antennas, SRM and VQM have better performance than the other two cases as shown in Fig. 8 and Table V; however, the performance gain is minor. As in the single-beam case at the source, the achieved aggregated

video quality is limited by the capacity between relays and a destination.

B. Expectation of Achieved Aggregated Video Quality

This section evaluates the performance of VQM in terms of expected achieved aggregated video quality. We varied the numbers of sources and relays from 0 to 15 with 4 steps, i.e., 0, 5, 10, 15. Then, the expectation of achieved aggregated video quality is obtained for the given numbers of sources and relays. The result of the single-beam antennas at sources and relays case is presented at Fig. 9(a) and Table VI. Similarly the results of the other two cases are presented at Fig. 9(b)/Fig. 9(c) and Table VII/Table VIII.

As shown in these three figures and tables, if we allow more beams to relays or sources, then we can obtain more video qualities. In addition, if we have more relays or sources, then we can have more aggregated video qualities.

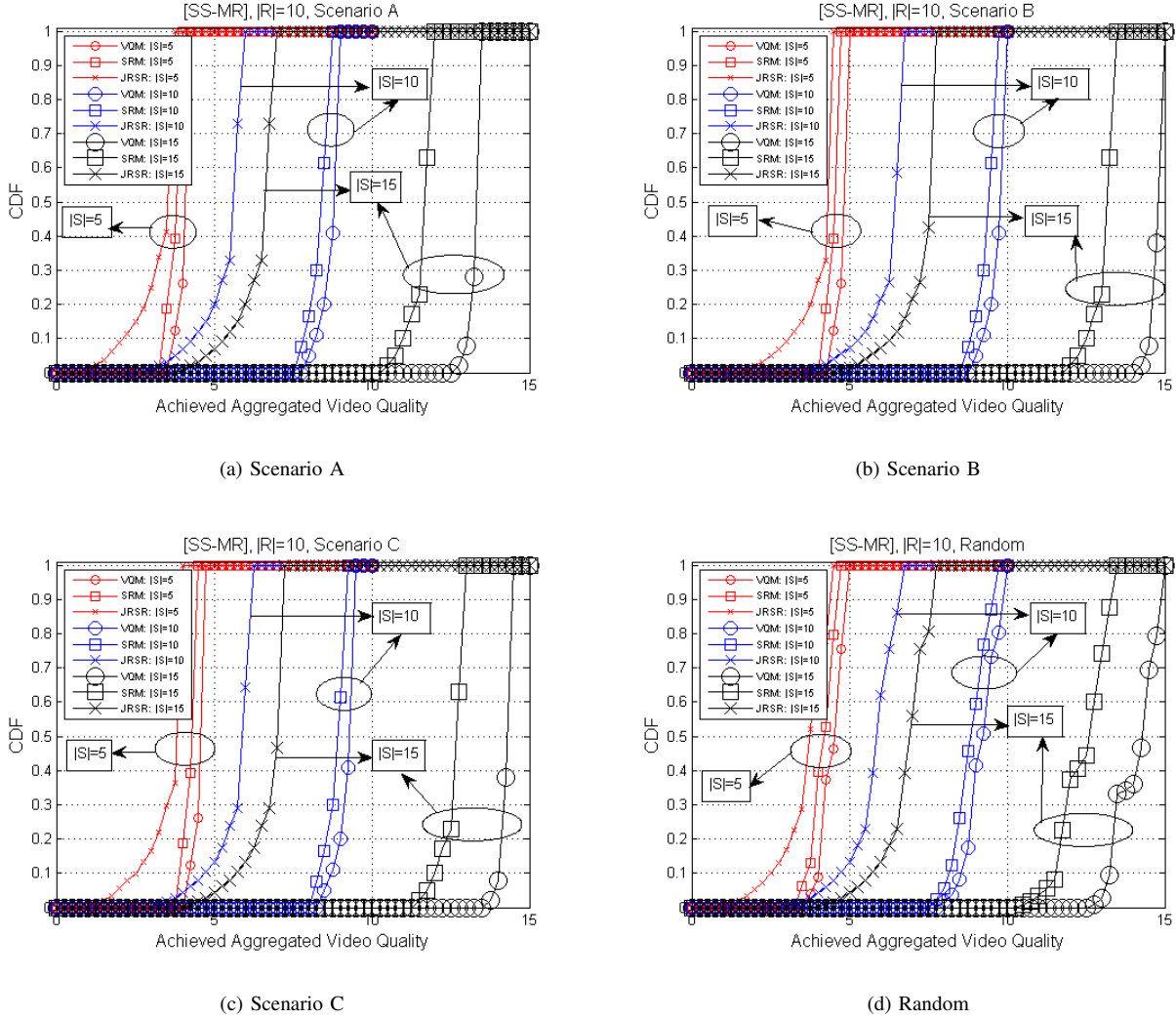


Fig. 7. Simulation Result for Single-Beam Antennas at Sources and Multiple-Beam Antennas at Relays: Various Number of Sources ($|S| = 5, 10, 15$) and Fixed Number of Relays ($|R| = 10$)

C. Impact of Lower Bound Setting

In previous simulation, the lower bounds for the data rate per data stream (corresponding to the desired lower bound on the video quality) are set as 0.75 Gbit/s. In this section, we vary now this lower bound values from 0 Gbit/s (i.e., there is no lower bound setting) up to 1.5 Gbit/s (i.e., we allow only uncompressed HD video transmission) in steps of 0.1 Gbit/s. As a performance quality measure we define "stream outage", i.e., the probability that at least one stream does not have the minimum required quality. Obviously, this outage has to increase (and thus its complement, the probability of successful transmission, has to decrease) as the minimum video quality increases. We furthermore anticipate that VQM will be better able to handle the increased requirements, as it is more flexible.

This evaluation is performed for the case of single-beam antennas at the sources and multiple-beam antennas at relays when $|S| = 10, |R| = 15$ in Fig. 10.

As shown in Fig. 10, the case of relay deployment with

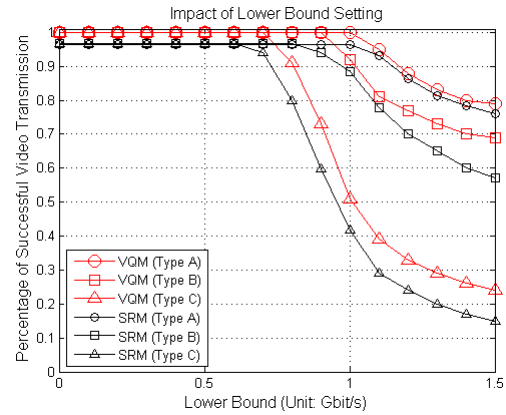


Fig. 10. Simulation Result for Various Lower Bound Setting: Single-Beam Antennas at Sources and Multiple-Beam Antennas at Relays, $|S| = 10, |R| = 15$

Scenario C suffers significantly from the higher required per-

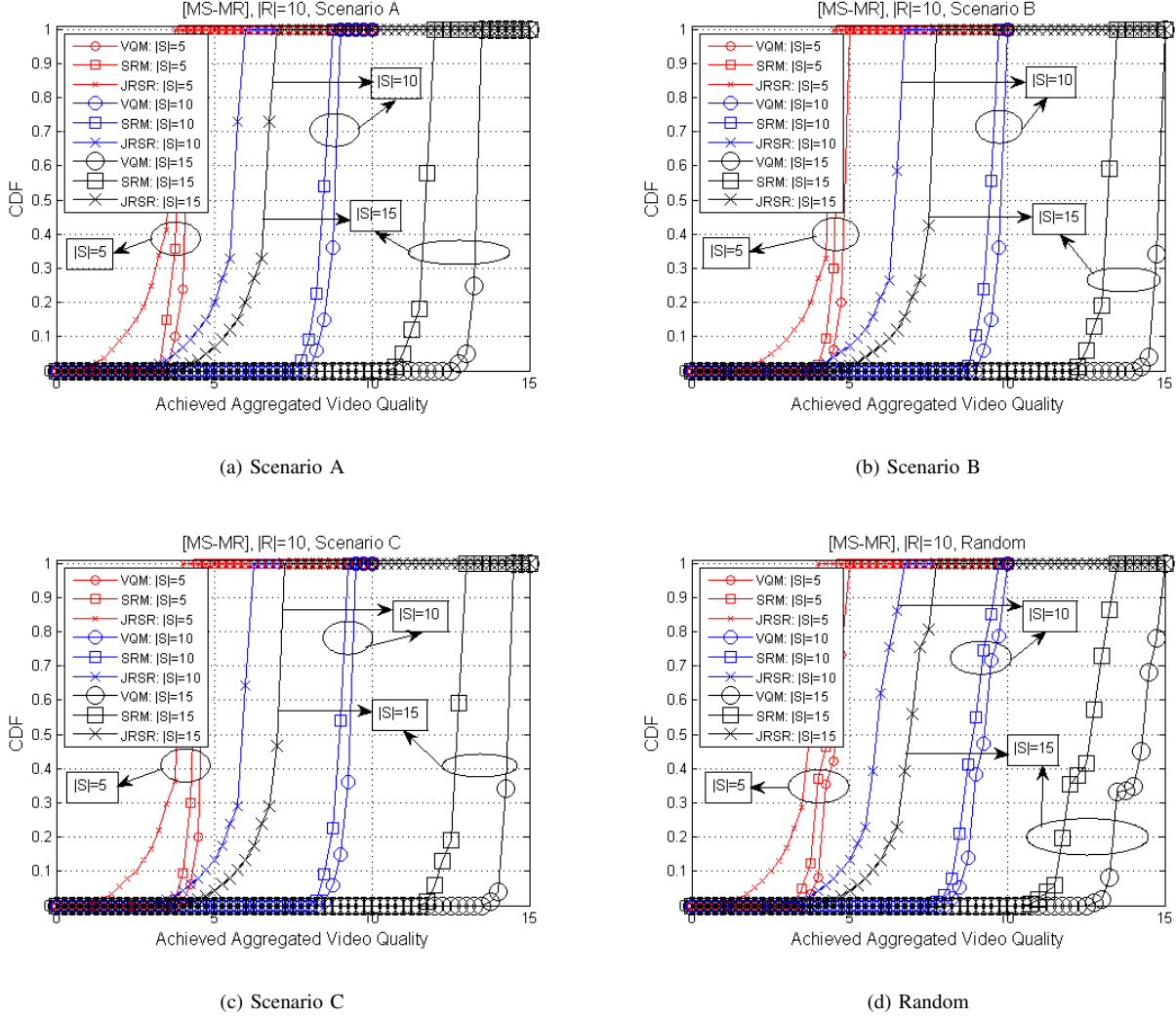


Fig. 8. Simulation Result for Multiple-Beam Antennas at Sources and Relays: Various Number of Sources ($|\mathcal{S}| = 5, 10, 15$) and Fixed Number of Relays ($|\mathcal{R}| = 10$)

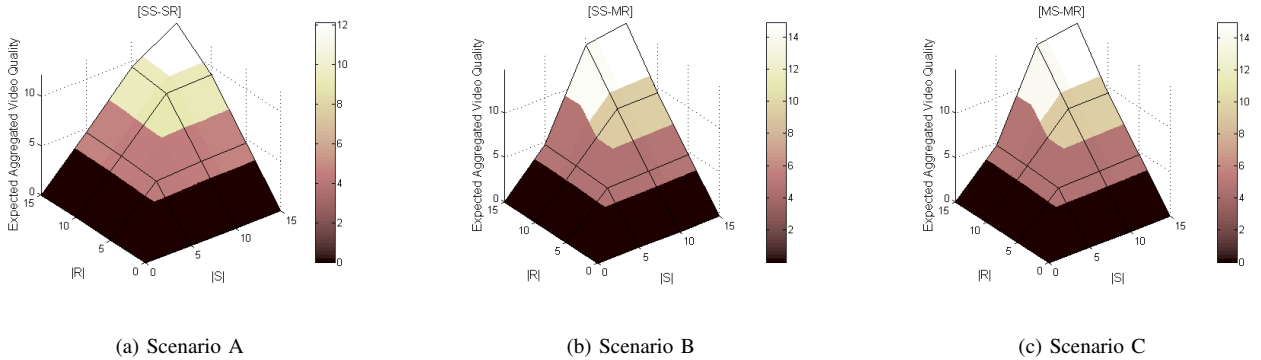


Fig. 9. Simulation Result for Expectation of Achieved Aggregated Video Quality

stream quality. With Scenario C relay deployment, the data rates between sources and relays are lower than the other cases. Thus, when we set the lower bound quite high, then all flows are disconnected. Thus, it achieves the lowest performance. On the other hand, in Scenario A relay deployment, all flows

between sources and relays have enough capacity to support uncompressed video transmission, thus, a higher setting for minimum quality does not have such a strong impact. In addition, Fig. 10 shows that VQM has better performance than SRM for all possible three types of relay deployment. For

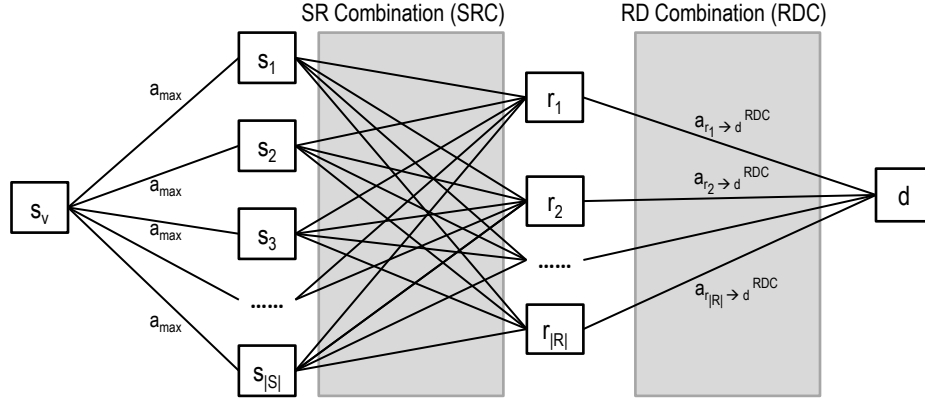


Fig. 11. Network Flow Model for the Multiple-Beam Antennas at Sources and Relays Case (Sum Rate Maximization)

TABLE IV
EXPECTATION OF ACHIEVED AGGREGATED VIDEO QUALITY FOR
SINGLE-BEAM ANTENNAS AT SOURCES AND MULTIPLE-BEAM
ANTENNAS AT RELAYS CASE

$ S $	$ R $	Scenario	VQM	SRM	JRSR
5	10	A	4.1531	3.8547	3.3313
5	10	B	4.9231	4.6047	4.1650
5	10	C	4.6531	4.3547	3.6315
5	10	Random	4.5698	4.2714	3.6534
10	5	A	4.1580	3.8620	3.3522
10	5	B	4.9480	4.6120	4.1817
10	5	C	4.6580	4.3620	3.6499
10	5	Random	4.5746	4.2786	3.6707
10	10	A	8.8075	8.4613	5.4825
10	10	B	9.8077	9.4613	6.3360
10	10	C	9.3081	8.9613	5.7946
10	10	Random	9.2894	8.9613	5.2044
10	15	A	8.8633	8.5450	5.6326
10	15	B	9.8633	9.5450	6.4561
10	15	C	9.3633	9.0450	5.9267
10	15	Random	9.3631	9.0432	5.8532
15	10	A	13.4050	11.7000	6.4825
15	10	B	14.8800	13.2001	7.3760
15	10	C	14.3801	12.7103	6.8386
15	10	Random	14.2217	12.5333	6.8510

more details, the average normalized video quality for VQM is 0.9531, 0.9138, 0.7288 for Scenario A, B, C, respectively. SRM cannot achieve maximum aggregated video quality due to the fact that it maximize the overall data rates instead of overall delivered video qualities.

VII. CONCLUDING REMARKS

This paper addresses a joint scalable coding and routing scheme for a 60 GHz millimeter-wave HD video streaming in an outdoor sports stadium broadcasting system. In the system, there are multiple wireless HD video cameras distributed throughout the stadium. To transmit the HD video data from the cameras over the wireless channels in a real-time manner, 60 GHz wireless links are used because they can exploit multi-

TABLE V
EXPECTATION OF ACHIEVED AGGREGATED VIDEO QUALITY FOR
MULTIPLE-BEAM ANTENNAS AT SOURCES AND RELAYS CASE

$ S $	$ R $	Scenario	VQM	SRM	JRSR
5	10	A	4.1656	3.8734	3.3313
5	10	B	4.9344	4.6469	4.1650
5	10	C	4.6813	4.3969	3.6315
5	10	Random	4.5938	4.3057	3.6534
10	5	A	4.1638	3.8707	3.3522
10	5	B	4.9536	4.6203	4.1817
10	5	C	4.6638	4.3707	3.6499
10	5	Random	4.5804	4.2873	3.6707
10	10	A	8.8125	8.4513	5.4825
10	10	B	9.8173	9.4516	6.3360
10	10	C	9.3123	8.9583	5.7946
10	10	Random	9.3141	8.8513	5.2044
10	15	A	8.8826	8.5739	5.6326
10	15	B	9.8724	9.5632	6.4561
10	15	C	9.3826	9.0738	5.9267
10	15	Random	9.3823	9.0739	5.8532
15	10	A	13.4203	11.7650	6.4825
15	10	B	14.9024	13.2548	7.3760
15	10	C	14.4025	12.7551	6.8386
15	10	Random	14.2417	12.5917	6.8510

TABLE VI
EXPECTATION OF ACHIEVED AGGREGATED VIDEO QUALITY FOR
SINGLE-BEAM ANTENNAS AT SOURCES AND RELAYS CASE (SEC. VI-B)

	$ S = 0$	$ S = 5$	$ S = 10$	$ S = 15$
$ R = 0$	0	0	0	0
$ R = 5$	0	4.2303	4.4958	4.5978
$ R = 10$	0	4.4912	9.0761	9.4560
$ R = 15$	0	4.5932	9.2508	12.1430

TABLE VII

EXPECTATION OF ACHIEVED AGGREGATED VIDEO QUALITY FOR SINGLE-BEAM ANTENNAS AT SOURCES AND MULTIPLE-BEAM ANTENNAS AT RELAYS CASE (SEC. VI-B)

	$ S = 0$	$ S = 5$	$ S = 10$	$ S = 15$
$ \mathcal{R} = 0$	0	0	0	0
$ \mathcal{R} = 5$	0	4.4301	4.5880	4.6900
$ \mathcal{R} = 10$	0	4.5764	9.3078	14.2217
$ \mathcal{R} = 15$	0	4.6784	9.3633	14.9110

TABLE VIII

EXPECTATION OF ACHIEVED AGGREGATED VIDEO QUALITY FOR MULTIPLE-BEAM ANTENNAS AT SOURCES AND RELAYS CASE (SEC. VI-B)

	$ S = 0$	$ S = 5$	$ S = 10$	$ S = 15$
$ \mathcal{R} = 0$	0	0	0	0
$ \mathcal{R} = 5$	0	4.4570	4.5937	4.6957
$ \mathcal{R} = 10$	0	4.5938	9.3140	14.2417
$ \mathcal{R} = 15$	0	4.6958	9.3792	14.9610

Gbit/s wireless data transmission. However, according to the high path loss of 60 GHz links, relays are used to extend communication coverage. We presented an algorithm for finding the combination of wireless link pairs between wireless HD video cameras and relays that can maximize the overall or per-flow video qualities of delivered HD video streams to one single broadcasting center. This paper considers three kinds of cases, i.e., single-beam antennas at sources and relays, single-beam antennas at sources and multiple-beam antennas at relays, and finally, multiple-beam antennas at sources and relays. For each cases, the given problem is initially formulated as non-convex MINLP and it is re-formulated as convex program, which allow optimum solutions.

We demonstrated that our algorithm outperforms algorithms based on sum-rate maximization and other well-known methods in the literature with various relay deployment scenarios, various number of sources, and various number of relays. According to the cumulative probability distribution plotting results depends on the achieved aggregated video quality, we verified that our proposed scheme achieves the best performance than the others.

REFERENCES

- [1] P. Smulders, "Exploiting the 60 GHz Band for Local Wireless Multimedia Access: Prospects and Future Directions," *IEEE Communications Magazine*, 40(1):140-147, January 2002.
- [2] H. Singh, J. Oh, C. Kweon, X. Qin, H.-R. Shao, and C. Ngo, "A 60 GHz Wireless Network for Enabling Uncompressed Video Communication," *IEEE Communications Magazine*, (46)12:71-78, December 2008.
- [3] WirelessHD: <http://wirelesshd.org>
- [4] Wireless Gbit Alliance (WiGig): <http://wirelessgbitalliance.org>
- [5] IEEE 802.15.3c Millimeter-wave-based Alternative Physical Layer Extension; <http://www.ieee802.org/15/pub/TG3c.html>, October 2009.
- [6] IEEE 802.11ad VHT Draft Version 5.0: http://www.ieee802.org/11/Reports/tgad_update.htm
- [7] H. Su and X. Zhang, "Joint Link Scheduling and Routing for Directional-Antenna Based 60 GHz Wireless Mesh Networks," in *Proceedings of IEEE Global Communications Conference (GLOBECOM)*, Honolulu, HI, USA, December 2009.
- [8] A.F. Molisch, *Wireless Communications*, 2nd Edition, Wiley-IEEE, February 2011.
- [9] Comotech Corporation; <http://www.comotech.com/en/index.html>
- [10] Millitech; <http://www.millitech.com/>
- [11] M.-C. Hwang, J.-H. Kim, D.T. Duong, and S.-J. Ko, "Hybrid Temporal Error Concealment Methods for Block-Based Compressed Video Transmission," *IEEE Transactions on Broadcasting*, 54(2):198-197, June 2008.
- [12] L. Zhou, B. Geller, B. Zheng, A. Wei, and J. Cui, "System Scheduling for Multi-Description Video Streaming Over Wireless Multi-Hop Networks," *IEEE Transactions on Broadcasting*, 55(4):731-741, December 2009.
- [13] H. Zhai, X. Chen, and Y. Fang, "Improving Transport Layer Performance in Multihop Ad Hoc Networks by Exploiting MAC Layer Information," *IEEE Transactions on Wireless Communications*, 6(5):1692-1701, May 2007.
- [14] J. Kim, Y. Tian, A.F. Molisch, and S. Mangold, "Joint Optimization of HD Video Coding Rates and Unicast Flow Control for IEEE 802.11ad Relaying," in *Proceedings of the 22nd IEEE International Symposium on Personal Indoor and Mobile Radio Communications (PIMRC)*, Toronto, Canada, 11 - 14 September 2011.
- [15] C. Cordeiro, D. Akhmetov, and M. Park, "IEEE 802.11ad: Introduction and Performance Evaluation of the First Multi-Gbps WiFi Technology," in *Proceedings of the 1st ACM International Workshop on mmWave Communications: from Circuits to Networks (mmCom)*, Chicago, IL, 2010.
- [16] H.L. Cycon, V. George, G. Hege, D. Marpe, M. Palkow, T.C. Schmidt, and M. Wahlsch, "Adaptive Temporal Scalability of H.264-compliant Video Conferencing in Heterogeneous Mobile Environments," in *Proceedings of IEEE Global Communications Conference (GLOBECOM)*, Miami, FL, USA, 6 - 10 December 2010.
- [17] M.-P. Kao and T.Q. Nguyen, "Rate-Distortion Optimized Bitstream Extractor for Motion Scalability in Wavelet-Based Scalable Video Coding," *IEEE Transactions on Image Processing*, 19(5):1214-1223, May 2010.
- [18] C.-Y. Tsai and H.-M. Hang, "Rate-Distortion Model for Motion Prediction Efficiency in Scalable Wavelet Video Coding," in *Proceedings of the IEEE Packet Video Workshop*, Seattle, WA, USA, 11 - 12 May 2009.
- [19] J. Cao and C. Williamson, "Towards Stadium-Scale Wireless Media Streaming," *Proceedings of the 14th IEEE International Symposium on Modeling, Analysis, and Simulation of Computer and Telecommunication Systems (MASCOTS)*, Monterey, CA, USA, 11-14 September 2006.
- [20] M.M. Akbar, M.S. Rahman, M. Kaykobad, E.G. Manning, and G.C. Shojha, "Solving the Multidimensional Multiple-Choice Knapsack Problem by Constructing Convex Hulls," *Computers and Operations Research*, vol. 33, pp. 1259 - 1273, 2006.
- [21] R.K. Ahuja, T.L. Magnanti, and J.B. Orlin, *Network Flows: Theory, Algorithms, and Applications*, Prentice Hall, 1993.
- [22] S. Boyd and L. Vandenberghe, *Convex Optimization*, Cambridge University Press, 2004.
- [23] S. Leyffer, A. Sartenaer, and E. Wanufelle, "Branch-and-Refine for Mixed-Integer Nonconvex Global Optimization," *Technical Report, Mathematics and Computer Science Division, Argonne National Laboratory*, 2008; Preprint ANL/MCS-P1547-0908.
- [24] J. Munkres, "Algorithms for the Assignment and Transportation Problems," *Journal of the Society for Industrial and Applied Mathematics*, 5(1):32-38, March 1957.
- [25] M. Grant and S. Boyd, *CVX: Matlab Software for Disciplined Convex Programming*, Version 1.21, April 2011.
- [26] M.-H. Lu, P. Steenkiste, and T. Chen, "Time-Aware Opportunistic Relay for Video Streaming over WLANs," in *Proceedings of IEEE International Conference on Multimedia and Expo (ICME)*, Beijing, China, 2 - 5 July 2007.
- [27] S. Mao, X. Cheng, Y.T. Hou, H.D. Sherali, and J. Reed, "On Joint Routing and Server Selection for MD Video Streaming in Ad Hoc Networks," *IEEE Transactions on Wireless Communications*, 6(1):338-347, January 2007.
- [28] W. Wei and A. Zakhori, "Interference Aware Multipath Selection for Video Streaming in Wireless Ad Hoc Networks," *IEEE Transactions on Circuits and Systems for Video Technology*, 19(2):165-178, February 2009.
- [29] S. Murthy, P. Hegde, V. Parameswaran, B. Li, and A. Sen, "Improved Path Selection Algorithms for Multipath Video Streaming in Wireless Ad-Hoc Networks," in *Proceedings of the IEEE Military Communications Conference (MILCOM)*, Orlando, FL, USA, 29-31 October 2007.
- [30] D. Giustiniano, V. Vukadinovic, and S. Mangold, "Wireless Networking for Automated Live Video Broadcasting: System Architecture and Research Challenges," in *Proceedings of the IEEE International Symposium on a World of Wireless, Mobile and Multimedia Networks (WoWMoM)*, Lucca, Italy, 20 - 23 June 2011.

- [31] S. Sharma, Y. Shi, Y.T. Hou, H.D. Sherali, S. Kompella, and S.F. Midkiff, "Joint Flow Routing and Relay Node Assignment in Cooperative Multi-Hop Networks," *IEEE Journal on Selected Areas in Communications*, 30(2):254-262, February 2012.
- [32] S. Singh, R. Mudumbai, and U. Madhow, "Interference Analysis for Highly Directional 60-GHz Mesh Networks: The Case for Rethinking Medium Access Control," *IEEE/ACM Transactions on Networking*, 19(5):1513-1527, October 2011.
- [33] Los Angeles Memorial Coliseum: <http://maps.google.com>

APPENDIX A

MAXIMUM FLOW FORMULATION

In the proposed scheme, the sum quality maximization is not considered because our aim is the maximization of achieved aggregated video quality and, in addition, the broadcasting center selects the meaningful video flows among the all incoming flows, therefore sum quality maximization is not meaningful in this application. However, in general cases, if we consider sum quality maximization (i.e., if the broadcasting center wants to aggregate all incoming HD video streams), our problem can be solved by the Edmonds-Karp algorithm in multiple-beam antennas at sources and relays case because this problem is equivalent to the traditional maximum network flow problem as shown in Fig. 11. As figured in Fig. 11, s_v is additionally defined as a virtual source to start the flows. After that, all individual flows from s_v to s_i , $\forall i$, are limited by a_{\max} (the maximum data rate for the given sub-channel and this value is 2.16 Gbit/s respect to WiGig standardization), thus the wireless link capacities (i.e., achievable rates) between s_v and s_i , $\forall i$ are set to be all a_{\max} . The link capacities between relays r_j , $\forall j$ and destination d are defined as the achievable rates between the relays and destination, i.e., $a_{r_j \rightarrow d}^{\text{RDC}}$, $\forall j$ and these values are upper bounds for the corresponding links. The links between all sources s_i , $\forall i$ and all relays r_j , $\forall j$ are limited by the achievable rates, i.e., $a_{s_i \rightarrow r_j}^{\text{SRC}}$, $\forall i, \forall j$ and these values are upper bounds for the corresponding wireless links. With these configurations, running Edmonds-Karp algorithm finds the maximum achievable rate flows from all sources s_i , $\forall i$ towards one destination d via relays r_j , $\forall j$, in turn, the optimal solutions for the sum video quality maximization is obtained [21].